Background Separation Based on Dual-Weighted Robust Principle Component Analysis

Rui He
Institute of Robotics and Intelligent Systems School of Information Science and Engineering, Wuhan University of Science and Technology
Wuhan , China
herui@wust.edu.cn

Huasong Xing
Institute of Robotics and Intelligent Systems School of Information Science and Engineering, Wuhan University of Science and Technology
Wuhan , China
huasongxing@wust.edu.cn

Zhengqin Xu
Institute of Robotics and Intelligent Systems School of Machinery and Automation, Wuhan University of Science and Technology
Wuhan , China
xuzhengqin@wust.edu.cn

Zhen Tian
Institute of Robotics and Intelligent Systems School of Information Science and Engineering, Wuhan University of Science and Technology
Wuhan , China
tianzhen2000@wust.edu.cn

Shiqian Wu
Institute of Robotics and Intelligent Systems School of Information Science and Engineering, Wuhan University of Science and Technology
Wuhan , China
shiqian.wu@wust.edu.cn

Shoulie Xie
Signal Processing, RF & Optical Dept. Institute for Infocomm Research
A*STAR,Singapore
slxie@i2r.a-star.edu.sg

***Abstract*—Robust principal component analysis (RPCA) is a powerful tool for solving background separation problems. However, the popular RPCA model doesn't make useful of the prior rank information in the background separation application, which usually leads to poor performance. To solve this issue, a new dual-weighted robust principal component analysis (DWRPCA) is proposed based on the prior rank information of the low-rank matrix and the sparsity of the sparse matrix. The singular values are weighted to encourage the target rank constraint of the low-rank matrix, and the sparse matrix is reweighted to enhance its sparsity. Experimental results show that the proposed dual-weighted RPCA model leads to high accuracy of background separation, and high robustness for a variety of complex scenes, in comparison with the existing methods.**

Keywords—background subtraction, robust principal component analysis, low-rank matrix, sparsity.

I. Introduction

Background and foreground separation is the main research field in video and image processing, which aims to separate the foreground and background from a video or an image. The accuracy of the separation has a great influence on the performance of moving object detection [1], recognition [2], and classification [3]. In the past years, Gaussian model [4] and filtering methods [5] were used to judge whether each pixel belonged to the foreground or the background, which can handle simple foreground and background separation. However, these methods don't consider the structural characteristics of images. Hence most algorithms cannot separate foreground and background well in complex and dynamic scenes such as the interference of noise, illumination and shadow. Therefore, it is necessary to study more effective algorithms to increase the separation accuracy in complex scenes.

Robust principal component analysis (RPCA) [6] has been widely studied in the background and foreground separation. As shown in Fig. 1, each frame of a video sequence is pulled into a column of the matrix M first, then the background image sequence is represented by the low-rank matrix L and the foreground image sequence is represented by the sparse matrix S, finally they can be separated through the RPCA algorithm without inputting the clean background training sample. The famous RPCA proposed by Candès et al. [6] can be described as follows:

$$\min_{L,S} rank(L) + \lambda\|S\|_0 \ \ s.t. M = L + S \tag{1}$$

where $M \in \mathbb{R}^{m\times n}$ is the observed image sequence, $rank(\cdot)$ denotes the rank function, $\|\cdot\|_0$ denotes the ℓ_0-norm and λ is the relative weight to trade off the two terms. However, Eq. (1) is an NP-hard problem due to the rank function and ℓ_0-norm [7][8].

Fig. 1. llustration of RPCA for foreground and background separation.

To solve the problem, Candès et al. [6] proposed an approximated model of the problem (1) with nuclear norm minimization (NNM) as follows:

$$\min_{L,S} \|L\|_* + \lambda\|S\|_1 \ \ s.t. M = L + S \tag{2}$$

where $\|L\|_* = \sum_1^{\min(m,n)} \sigma_i(L)$ denotes the nuclear norm of L which is the sum of all singular values, $\sigma_i(L)$ denotes the i-th singular value of L, and $\|\cdot\|_1$ denotes the ℓ_1-norm. In RPCA, the nuclear norm minimization is involved, and it can be solved by singular value soft-thresholding operation [9][10] on the observation matrix. That is

$$\begin{aligned}\hat{L} &= Prox_\tau(L) = arg\ \min_X \|M-L\|_F^2 + \tau\|L\|_* \\ &= US_\tau(\Sigma)V^T\end{aligned} \tag{3}$$

This work was supported in part by the National Natural Science Foundation of China under Grants 51805386, 61775172, and Hubei Key Technical Innovation Project under Grant ZDCX2019000025.

2021 IEEE 16th Conference on Industrial Electronics and Applications (ICIEA) | 978-1-6654-2248-2/21/$31.00 ©2021 IEEE | DOI: 10.1109/ICIEA51954.2021.9516373

where τ is a positive constant, $M = U\Sigma V^T$ is the SVD of M, and $S_\tau(\Sigma)$ is the soft-thresholding function with diagonal matrix $\Sigma = \text{diag}(\sigma_{i_{1\le i\le min(m,n)}})$. The diagonal element $S_\tau(\Sigma)_{ii}$ is given by

$$S_\tau(\Sigma)_{ii} = sgn(\sigma_i) \cdot max(|\sigma_i| - \tau, 0). \quad (4)$$

It can be seen that all singular values in the nuclear norm minimization are reduced by the same scale τ. Candès et al. proved that the solution of problem (2) is consistent with that of the original NP-hard problem (1), and inexact augmented Lagrange multipliers (IALM) [11] have been proved to be efficient and effective in solving the problem (2).

RPCA can handle simple background and foreground separation problem. However, the basic assumptions of RPCA are often violated in the complex background or foreground scenes, for example, the very subtle movement of the foreground objects. Since the foregrounds are highly correlated, the sparse components don't conform to a random and independent distribution. Therefore the low-rank structure of L can't be approximated well. It is easy to produce ghost images in the separated background by using RPCA. Therefore, there are still some shortcomings in RPCA for background and foreground separation.

Recently, a few of RPCA variants have been developed to use in various scenes. Oh et al. **Error! Reference source not found.** proposed a minimization of partial sum of singular values (PSSV) based on the prior rank information of the data matrix. A very clean background can be separated by PSSV. However, the PSSV algorithm is not suitable for large-scale video surveillance applications. Gu et al. [12] proposed a weighted nunclear norm minimization model (WNNM) based on the singular values. However, a lot of parameters need to be adjusted continuously, which is not applicable in practical applications. Xue et al. [13] combined truncated nuclear norm [15] and sparse regularization (TNNSR) to propose an optimization model for increasing the estimation accuracy, but the computational complexity of the algorithm is so large that it is difficult to apply to practical image processing problems. Peng et al. [16] proposed a reweighted nuclear norm in RPCA for robust image restoration.

In this paper, we propose an improved RPCA method to perform the background and foreground separation in complex scenes. In our method, dual weights are incorporated into RPCA model based on the prior rank information of the low-rank matrix and the sparsity of the sparse matrix. The proposed model can enhance the low-rank property of the recovered low-rank matrix and the sparsity of the recovered sparse matrix. The experimental results also show that the improved model can get a more accuracy and robust performance in various complex scenes.

II. Dual-Weighted RPCA

A. Low-rank weights

In the classical RPCA algorithm, the singular values are all contracted with τ as the threshold shown in (4). However, the singular values have clear physical meanings, so different singular values should be treated differently [12]. The larger singular values include the more important information of the data matrix and should be shrunk less. If the rank of the data matrix is known, a suitable weighted nuclear norm minimization (WNNM) is a good model to improve performance of RPCA:

$$\min_{L,S} \|L\|_{w_L,r} + \lambda\|S\|_1, \ s.t. M = L + S \quad (5)$$

where $w_L = [w_{L,1}, \ldots, w_{L,n}]^T$ with $w_i > 0$ denotes the non-negative weight, r denotes the target rank of matrix L that is known in background and foreground separation applications, for instance, $r=1$ for simple background subtraction (If there are lighting changes, the rank scale can be appropriately increased). In [12], the rank of matrix L was assumed to be considerable low, but it was unknown. In fact the weighted value w_i was related to the singular value of the low-rank matrix where smaller weights were assigned to the larger singular values [13].

Since the first few singular values of the largest matrix account for more than 99% of the sum of all singular values, it is necessary to reduce the weights corresponding to the first few singular values. Therefore, we proposed a special case of WNNM model based on the rank r. The weight coefficient w is set as follows:

$$w_{L,i} = \begin{cases} 0 & if\ i \le r \\ +\infty & otherwise \end{cases} \quad (6)$$

The first r weights are set to 0 and the other weights are set to $+\infty$ in order to approximate the rank function of the matrix.

The weighting strategy in Eq. (6) strengthens the rank constraint of the low-rank matrix and encourages the rank of the recovered low-rank matrix to be equal to the target rank r. In fact in original WNNM, when the singular values of the target matrix are very small, the low-rank matrix L recovered by minimizing the nuclear norm is a rank-deficient matrix, that is, the rank of the recovered low-rank matrix is less than r. In contrast, the proposed weighting method in Eq. (6) does not minimize the space of matrix L within the target rank, low-rank space estimation for matrix L has no bias. Moreover, when the singular value of the target matrix is very large, the low-rank matrix can also be estimated accurately by using (6).

B. The sparse weights

Although the weighted RPCA model (5) can strengthen the rank constraint of the low-rank matrix, it also affects the sparsity of the recovered sparse matrix during the iterative process. To improve the recovery quality of the sparse matrix, here we propose a dual-weighted RPCA model based on the weighted model (5). The sparse weighting technique was originally proposed by Candès et al. [16], which can enhance the sparsity of the sparse vector. Sparse weighting is also called reweighted ℓ_1-norm defined as $\|w \cdot \mathbf{x}\|_1$, where $\mathbf{x} = \{x_i\} \in \mathbb{R}^n$, $w = \{w_i\} \in \mathbb{R}^n$ and $w_i \ge 0$ denotes the weight of each entry of $\mathbf{x}$. The weight w_i is inversely proportional to the absolute value of the corresponding $\mathbf{x}$ entry, i.e., $w_i = \frac{1}{|x_i|}$(for $x_i \neq 0$). For the weight matrix w and data matrix $\mathbf{x}$, it is obvious that the formula $\|w \odot \mathbf{x}\|_1 = \|\mathbf{x}\|_0$, where $\odot$ denotes the Hadamard product and $\|\cdot\|_0$ denotes the pseudo-ℓ_0 norm (the number of nonzero entries). If the reweighted ℓ_1-norm is applied in RPCA, we have the following optimization problem:

$$\min_{L,S} \|L\|_* + \lambda\|w_s \odot S\|_1, s.t. M = L + S \quad (7)$$

where $w_s = \{w_{s,i}\} \in \mathbb{R}^{m\times n}$ and $w_{s,i} \geq 0$ denote the weight of each entry S_{ij} of the sparse matrix S, i.e., $w_{s,i} = \frac{1}{|S_{ij}|+\varepsilon}$ (ε is very small positive constant to avoid dividing by zero). In the RPCA model (7), the use of the sparse weighted model can not only enhance the sparsity of the sparse matrix but also reduce the recovery error.

C. Dual-weighted RPCA and its solutions

By combining the weighted low-ranks and the reweighted ℓ_1-norm, we can obtain a new optimization model as follows:

$$\min_{L,S} \|L\|_{w_L,r} + \lambda\|w_S \odot S\|_1, \ s.t. M = L + S \tag{8}$$

This model is named dual-weighted robust principal component analysis (DWRPCA). The optimization problem (8) can be efficiently solved via alternating direction minimization of multipliers (ADMM) algorithm. First, the augmented Lagrangian function of (8) can be written as:

$$\mathcal{L}(L,S,Y) = \|L\|_{w_L,r} + \lambda\|w_S \odot S\|_1 + \langle Y, M - S - L\rangle + \frac{1}{2}\mu\|M - L - S\|_F^2 \tag{9}$$

where $Y \in \mathcal{R}^{m\times n}$ denotes the augmented Lagrangian multiplier matrix, $\langle\cdot,\cdot\rangle$ represents matrix inner product, μ is the positive penalty scalar and $\|.\|_F$ denotes the Frobenius norm. Since model (9) has three variables (*L, S*, and *Y*), we can update each variable by fixing other variables at each iteration. Thus the optimization problem (9) can be divided into the following three sub-problems:

***S** sub-problem*: By fixing *L* and *Y,* variable *S* is determined by

$$\begin{aligned} S^* &= \min_S \lambda\|w_S \odot S\|_1 + \langle Y, M - S - L\rangle + \frac{1}{2}\mu\|M - L - S\|_F^2 \\ &= \min_S \frac{\lambda}{\mu}\|w_S \odot S\|_1 + \frac{1}{2}\|S - (M - L + \mu^{-1}Y)\|_F^2 \\ &= \mathcal{S}_{\frac{\lambda w}{\mu}}[M - L + \mu^{-1}Y] \end{aligned} \tag{10}$$

where the non-uniform soft threshold operator S_W can be defined as follows [11,12].:

$$S_W\{X\} = \{sign(x_i)max(|x_i| - w_i),0\} \tag{11}$$

with $X = \{x_i\}_{i=1}^n \in R^n, W = \{w_i\}_{i=1}^n \in R_{++}^n$. Obviously it is the closed-form solution, hence it is very efficient to solve the reweighted ℓ_1-norm minimization by the non-uniform soft threshold operator.

***L** sub-problems*: While *S* and *Y* are fixed, we can obtain *L* by solving the following optimization problem:

$$\begin{aligned} L^* &= \min_L \|L\|_{w_L,r} + \langle Y, M - S - L\rangle + \frac{1}{2}\mu\|M - L - S\|_F^2 \\ &= \min_L \frac{1}{2}\|L\|_{w_L,r} + \|L - (M - S + \mu^{-1}Y)\|_F^2 \\ &= US_{w\tau}(\Sigma)V^T \end{aligned} \tag{12}$$

where $U\Sigma V^T = M - S + \mu^{-1}Y$ denotes the singular value decomposition, and the non-uniform soft threshold operator of the low-rank matrix is rewritten as:

$$S_{w\tau}(\Sigma)_{ii} = sgn(\sigma_i)\cdot max(|\sigma_i| - w_i\tau, 0) \tag{13}$$

In light of the low-rank matrix weights shown in Eq. (6), We can get the simplest formula for solving low-rank matrices as follows:

$$\hat{L} = H_r(M - S + \mu^{-1}Y) = U_r\Sigma_r V_r^T \tag{14}$$

Where Σ_r denote the first r singular values of matrix $M - S + \mu^{-1}Y$, i.e., $\Sigma_r = diag(\sigma_i, \ldots, \sigma_r)$. $H_r(\cdot)$ denotes the truncated SVD.

Y *sub-problems*: In the iterative process, *Y* can be updated by

$$Y_{k+1} = Y_k + \mu(M - L_{k+1} - S_{k+1}) \tag{15}$$

In summary, the ADMM-based solution to DWRPCA problem (8) can be shown in Algorithm 1.

Algorithm 1 DWRPCA

---

input: $\boldsymbol{M} \in \mathbb{R}^{m\times n}, \lambda, \mu, \rho$;
1: **initialization:** $\boldsymbol{S_0} = 0, L_0 = 0,, \boldsymbol{Y_0} = 1.25/\|M\|_2$ and w_L initialized by (6);
2: **while** not converged **do**
3: computer $\boldsymbol{S}_{k+1} = \mathcal{S}_{W_S\frac{\lambda}{\mu}}[\boldsymbol{M} - \boldsymbol{L}_k + \mu^{-1}\boldsymbol{Y}_k]$
4: computer $\boldsymbol{L}_{k+1} = \mathcal{H}_r[\boldsymbol{M} - \boldsymbol{S}_{k+1} + \mu^{-1}\boldsymbol{Y}_k]$
5: computer $\boldsymbol{Y}_{k+1} = \mu(\boldsymbol{M} - \boldsymbol{L}_{k+1} - \boldsymbol{S}_{k+1})$
6: update $W_S = 1./(\boldsymbol{S} + \varepsilon)$;
7: update $\mu = \min(\mu \times \rho, \mu \times 10^7)$
8: **end while**
9: **output:** $\boldsymbol{L}, \boldsymbol{S}$.

In the above algorithm, the iteration is terminated when $\frac{\|M - S_k - L_k\|_F}{\|D\|_F} < 10^{-4}$.

III. Experimental Results

In order to evaluate the performance of the proposed DWRPCA method, here we consider the following video sequences: Bootstrap, ForegroundAperture, TimeOfDay, busStation, and ArchSequence. The first three videos include 2000 frames with image size 160×120, busStation video contains 1250 frames with image size 360×240, and ArchSequence have 5 pictures only with image size 669×1024. The datasets include scenarios with different sample sizes, lighting changes, and slow movement, which can evaluate the performance of the image processing algorithm comprehensively.

In this section, for performance comparison, we choose the most representative methods: RPCA [6], PSSV **Error! Reference source not found.**, RPCA-GD [18], LRSD-TNNSR [13]. All methods use the same parameter settings. For example, $\lambda = 1/\sqrt{\max(m, n)}$, $\mu = 1.25/\max(\sigma_i(M))$, $\rho = 1.5$ and the termination condition is $\|M - L_k - S_k\|_F \leq 10^{-4}\|M\|_F$. All the codes are written in Matlab and all the experiments are conducted on a PC running Windows 10 OS with 32G RAM and 3.2GHz CPU.

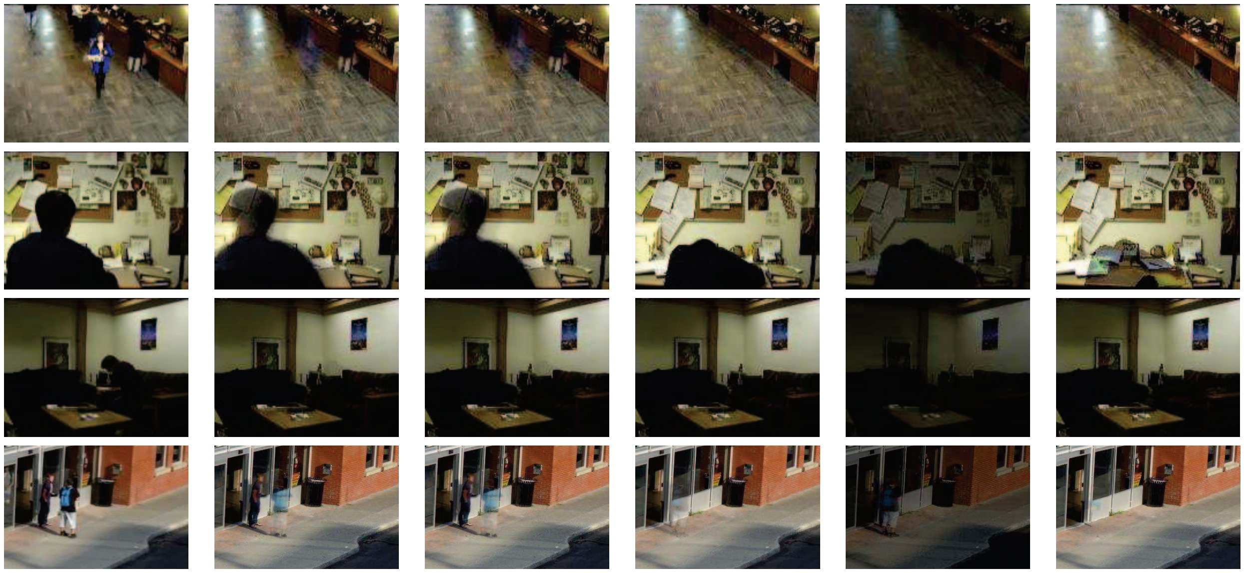

(a)Original **(b)RPCA** **(c)PSSV** **(d)RPCA-GD** **(e)LRSD-TNNSR** **(f)DWRPCA**

Fig. 2. The background separations of RPCA, PSSV, RPCA-GD, LRSD-TNNSR and DWRPCA on bootstrap, ForegroundAperture, TimeOfDay, and busStation.

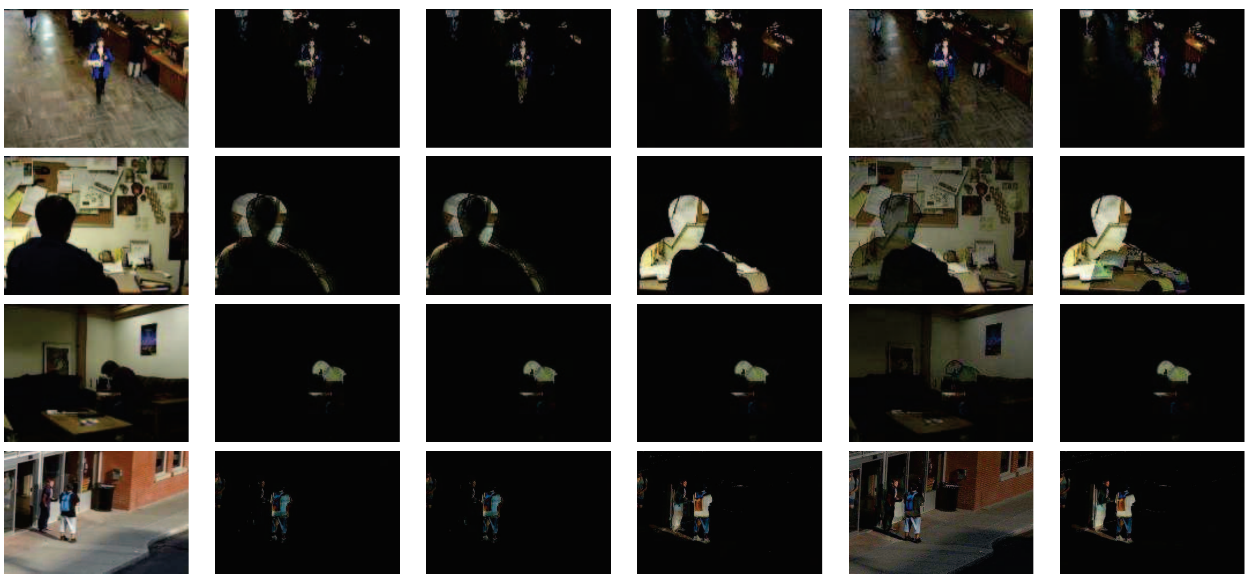

(a)Original **(b)RPCA** **(c)PSSV** **(d)RPCA-GD** **(e)LRSD-TNNSR** **(f)DWRPCA**

Fig. 3. The foreground separations of RPCA, PSSV, RPCA-GD, LRSD-TNNSR and DWRPCA on Bootstrap, ForegroundAperture, TimeOfDay, and busStation.

Fig. 2 shows the background separation results of video sequences. It can be seen that the DWRPCA algorithm is significantly better than other algorithms in terms of visual quality of the separated backgrounds. The backgrounds separated by PSSV and RPCA has obvious ghosts, the separation results of RPCA-GD and LRSD-TNNSR show obvious color and brightness distortion. The proposed DWRPCA algorithm achieves the clearest backgrounds. In particular, for the ForegroundAperture video sequences with slow foreground motion, it can also get quite clean background images.

Fig. 3 shows the foreground separation results of video sequences. It can be seen that the proposed DWRPCA can obtain the whole foreground moving objects. Moreover, the proposed DWRPCA algorithm can also achieve good separation results even though there are insufficient samples, which are shown in Fig. 4 for the foreground and background separation results of the ArchSequence dataset with 5 pictures only.

(a)Original (b)RPCA (c)PSSV

(d)RPCA-GD (e)LRSD-TNNSR (f)DWRPCA

Fig. 4. The background and foreground separations of RPCA, PSSV, RPCA-GD, LRSD-TNNSR and DWRPCA on ArchSequence.

In our experiments, we use the 'lansvd' routine from the PROPACK[1] library to get the singular value decomposition of the first r dimension of the matrix, which is adopted in the RPCA, PSSV and our proposed DWPRCA methods. The routine can solve SVD of a large-size matrix to accelerate the solution of L *sub-problems*. As shown in Table 1, the proposed DWRPCA algorithm is faster than other algorithms under the conducted experiments conditions.

In order to evaluate various background and foreground separation methods in numerical, the following measurement criteria are considered: recall, precision, and F-measure[19], which are defined as

$$recall = \frac{TP}{TP+FN} \tag{16}$$

$$precision = \frac{TP}{TP+FP} \tag{17}$$

$$F-measure = \frac{2\cdot recall\times precision}{rcall+precision} \tag{18}$$

where TP represents the number of all pixels in the foreground that are correctly separated; FN represents the number of the foreground pixels that are erroneously separated from the backgrounds; FP represents the number of background pixels that are erroneously separated.

Fig. 5 shows the binarization of the foreground images separated by RPCA, PSSV, RPCA-GD, and DWRPCA (due to the poor effect of LRSD-TNNSR in the foreground separation experiment, we didn't use it for comparison experiments). Table 2 shows the relevant evaluation indices of all methods. The proposed DWRPCA achieves the highest F-measure in almost video datasets except for TimeOfDay. Therefore, the proposed DWRPCA outperforms other methods in background and foreground separation.

TABLE I. CPU TIME (S) OF DIFFERENT ALGORITHMS AND DATASETS

Dataset	*RPCA*	*PSSV*	*RPCA-GD*	*LRSD-TNNSR*	*DWRPCA*
bootstrap	787	817	791	518	**104**
ForegroundAperture	797	824	844	623	**107**
TimeOfDay	792	801	816	557	**106**
busStation	1443	1452	1453	1565	**295**
ArchSequence	**4**	4	43	68	15

TABLE II. EVALUATION INDICES OF DIFFERENT ALGORITHMS AND DATASETS

Algorithm	*bootstrap*			*ForegroundAperture*			*TimeOfDay*			*busStation*		
	R	P	F	R	P	F	R	P	F	R	P	F
RPCA	0.36	0.94	0.52	0.38	0.57	0.46	0.73	0.79	0.76	0.96	0.29	0.45
PSSV	0.35	**0.94**	0.52	0.39	0.58	0.47	**0.73**	0.80	**0.76**	**0.96**	0.30	0.45
RPCA-GD	0.48	0.80	0.60	0.54	0.81	0.64	0.41	**0.99**	0.58	0.91	0.59	0.72
DWRPCA	**0.51**	0.72	**0.60**	**0.83**	**0.92**	**0.87**	0.66	0.83	0.73	0.93	**0.63**	**0.75**

1 http://sun.stanford.edu/~rmunk/PROPACK/

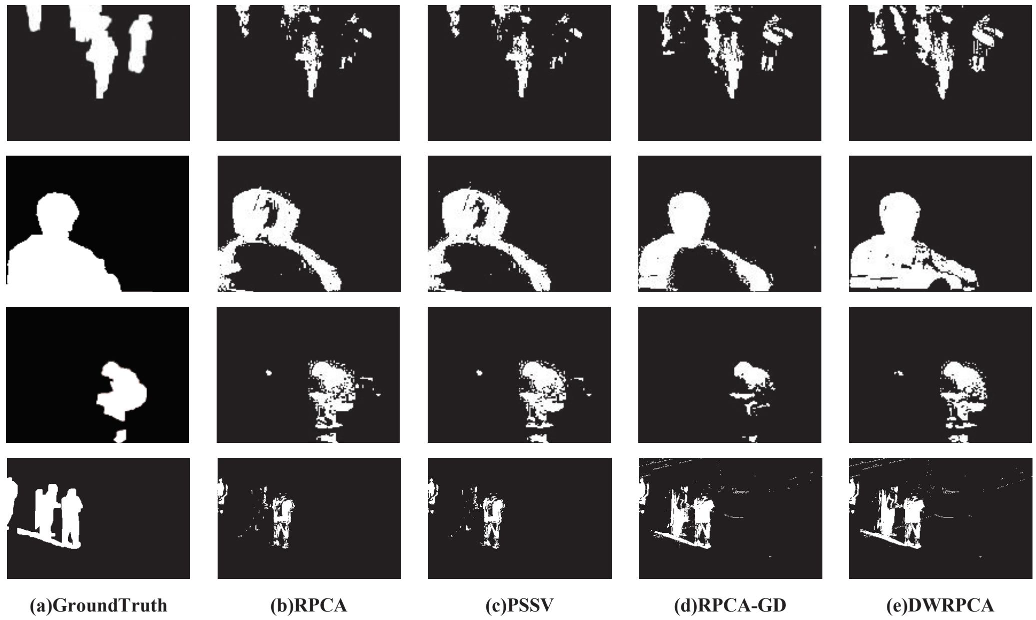

Fig. 5. Binarization of the foreground images of RPCA, PSSV, RPCA-GD and DWRPCA on Bootstrap, ForegroundAperture, TimeOfDay, and busStation.

IV. CONCLUSION

This paper presents a new RPCA algorithm for background and foreground separation. Based on the prior rank information of the target low-rank matrix and sparsity of sparse matrix, a dual-weighted optimization model is proposed for weighting low-rank and sparse components. This method can not only guarantee the low-rank structure of the estimated low-rank matrix, but also enhance the sparsity of the estimated sparse matrix. An efficient ADMM-based algorithm is presented to solve the optimization model. Experimental results also show that our proposed DWRPCA method outperforms other existing methods in background and foreground separation.

REFERENCES

[1] Z. Hu, Y. Wang, R. Su, X. Bian, H. Wei and G. He, "Moving object detection based on non-convex RPCA with segmentation constraint," in IEEE Access, vol. 8, pp. 41026-41036, 2020.

[2] T. Y. Chuang, J. Y. Han, D. J. Jhan and M. D. Yang. "Geometric recognition of moving objects in monocular rotating imagery using faster R-CNN," Remote Sens, vol. 12, no. 12,2020 , pp. 1908, 2020.

[3] J. Xu, L. Zhao, S. Zhang, C. Gong and J. Yang. "Multi-task learning for object keypoints detection and classification," Pattern Recognition Letters, vol. 130, pp. 182-188, 2020.

[4] Z. Zivkovic. "Improved adaptive Gaussian mixture model for background subtraction," International Conference on Pattern Recognition, vol. 2, pp. 28-31, 2004.

[5] A. El Maadi and X. Maldague, "Outdoor infrared video surveillance: A novel dynamic technique for the subtraction of a changing background of IR images," Infraredphysics & technology, vol. 49, no. 3, pp. 261–265, 2007.

[6] E. J. Candès, X. Li, Y. Ma and J. Wright. "Robust principal component analysis?" Journal of the ACM, vol. 58, no. 3, 2011, pp. 1-37, 2011.

[7] B. Recht, M. Fazel and P.A. Parrilo, "Guaranteed minimum-rank solutions of linear matrix equations via nuclear norm minimization," SIAM review, vol. 52, no. 3, pp. 471-501, 2010.

[8] T. Bouwmans, S. Javed, H. Zhang, Z. Lin and R. Otazo, "On the applications of robust PCA in image and video Processing," Proceedings of the IEEE, vol. 106, no. 8, pp. 1427-1457, 2018.

[9] K. C. Toh and S. Yun. "An accelerated proximal gradient algorithm for nuclear norm regularized least squares problems," Pacific Journal of Optimization, vol. 6, no. 3, pp. 615-640, 2010.

[10] J. F. Cai, E.J. Candès and Z. Shen. "A singular value thresholding algorithm for matrix completeon," SIAM Journal on Optimization, vol. 20, no. 4, pp.1956-1982, 2010.

[11] Z. Lin, M. Chen and Y. Ma, "The augmented lagrange multiplier method for exact recovery of a corrupted low-rank matrices," in UIUC Technical Report, 2009.

[12] T. H. Oh, Y. W. Tai, J. C. Bazin and H. Kim. "Partial sum minimization of singular values in robust PCA: algorithm and applications," IEEE Transactions on Pattern Analysis and Machine Intelligence, vol. 38, no.4, pp. 744-758, 2016.

[13] S. Gu, Q. Xie, D. Meng, W. Zuo and X. Feng. "Weighted nuclear norm minimization and its applications to low level vision," International Journal of Computer Vision, vol. 121, no. 2, pp. 183-208, 2017.

[14] Z. Xue, J. Dong, Y. Zhao, L. Chang, C. Ryad, "Low-rank and sparse matrix decomposition via the truncated nuclear norm and a sparse regularizer," The Visual Computer, vol. 35, no. 11, pp. 1549-1566, 2019.

[15] Y. Hu, D. Zhang, J. Ye, X. Li and X. He, "Fast and accurate matrix completion via truncated nuclear norm regularization," IEEE transactions on pattern analysis and machine intelligence, vol. 35, no. 9, pp. 2117-2130, 2013.

[16] Y. Peng, J. Suo, Q. Dai and W. Xu, "Reweighted low-rank matrix recovery and its application in image restoration," in IEEE Transactions on Cybernetics, vol. 44, no. 12, pp. 2418-2430, 2014.

[17] E. J. Candès, M. B. Wakin and S. P. Boyd, "Enhancing sparsity by reweighted ℓ_1 minimization," Journal of Fourier analysis and applications, vol.14, no.(5-6), pp. 877-905, 2008.

[18] X. Yi, D. Park, Y.Chen and C. Caramanis, "Fast algorithms for robust PCA via gradient descent," in advances in neural information processing systems, pp. 4152-4160, 2016.

[19] Y . Li, G. Liu, Q. Liu, Y. Sun and S. Chen, ''Moving object detection viasegmentation and saliency constrained RPCA,''Neurocomputing, vol. 323, pp. 352–362, 2019